Nanoscale

Accepted Manuscript

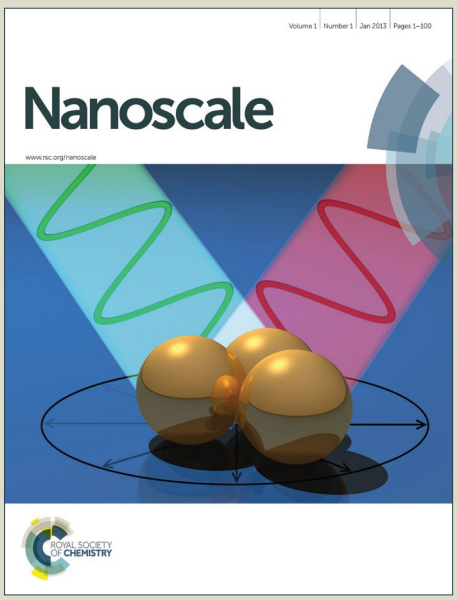

ROYAL SOCIETY OF CHEMISTRY

www.rsc.org/nanoscale

A versatile method to produce functionalized cellulose nanofiber and its application

Pei Huang, Yang Zhao, Shigenori Kuga, Min Wu*, Yong Huang*

Technical Institute of Physics and Chemistry, Chinese Academy of Sciences,
29 Zhongguancun East Road, Beijing, 100190 (China)
E-mail: wumin@mail.ipc.ac.cn

KEYWORDS: cellulose nanofiber, mechanochemical, surface esterification, anhydride

ABSTRACT: A facile method was developed to produce functionalized cellulose nanofiber in one step by ball milling. Through the synergism of mechanical and chemical actions, the produced cellulose nanofibers are *ca*. 20 nm wide and several micrometers long, with surface properties tailored by choice of modifying reagent. Modified by succinic anhydride, cellulose nanofiber shows enhanced hydrophilicity and can be readily dispersed in water or DMSO, and gives zeta potential of -38.7 mV due to carboxyl group on the surface. Modified by dodecyl succinic anhydride, cellulose nanofiber has excellent dispersibility in o-xylene and good compatibility with polyethylene. The polyethylene-cellulose nanofiber composite presents overall enhancement of mechanical properties. This method opens a new way to production of functionalized cellulose nanofiber.

Introduction

Cellulose nanofiber (including whiskers, i.e. disrupted ones) have a great deal of interest on account of its abundance, biodegradability, robust mechanical properties[1] and chemical tunability[2]. In last decades, the desire to release the environmental burden has boosted the application of cellulose nanofiber in many fields[3]. One of the intriguing application areas for cellulose nanofiber is the reinforcement of composites, in which cellulose nanofiber has proven its remarkable enhancement effects.

However, the hydrophilic surface limits the use of cellulose nanofiber to hydrophilic matrixes, such as starch[4], regenerated cellulose[5], and etc. To expand the application field, several approaches have been developed to improve the interface between nanofiber and hydrophobic matrix. The introduction of surfactant is one option, but may result in poor mechanical properties of nanocomposite[6]. To modify matrix with less hydrophobic[7] is another option, but it may sacrifice some characteristics of the polymer. Therefore, chemical modification of cellulose nanofiber is believed to be the most effective method for reinforcing nanocomposite[8]. However, the surface modification of cellulose nanofiber always involves complicated procedures or hazardous chemicals, hindering its scaled up production.

Recently, we reported a novel method of mechanochemical esterification by acyl chlorides, giving cellulose nanofibers with tailored surface properties, high dispersity and high aspect ratio[9]. However, the inherent hazard and toxicity of chlorides set a serious drawback in the application of cellulose nanofiber. In contrast, acyl anhydrides are milder and safer reagents for esterification. Cyclic anhydrides react with cellulose to form half-esters, introducing extra carboxyl groups to the nanofiber. Also, succinic anhydride is available as many derivatives with long-chain alkyl groups used in papermaking. Therefore, we here attempted to apply mechanochemical esterification by using this class of reagents to tune the surface property of cellulose nanofiber. The reaction medium also needs optimization. Dimethyl sulfoxide (DMSO) has greater swelling ability for cellulose than N,N-dimethylformamide (DMF)[10], but it could not be used for acid chloride due to the reactivity of DMSO. Thus we employed DMSO as reaction medium for two types of succinic anhydride for manipulating the hydrophilicity of cellulose nanofibers. The products were subjected to a series of characterizations.

Materials

The cellulose materials were cellulose microcrystalline (Sigma-Aldrich) and commercial hardwood pulp (New Zealand). These were dried in vacuum at 105 °C for 2 h before used. Esterifying agent, succinic anhydride (Alfa Aesar) and n-dodecyl succinic anhydride (TCI, Japan), catalyst dimethylaminopyridine (DMAP) (Alfa Aesar, USA) and low density polyethylene (51215B, Beijing Huaer Co., Ltd, China) were used as received. Acetone, ethanol, DMSO and o-xylene (Beijing Chemical Reagent, China) were used without further purification.

Experiment

Surface esterification by ball milling

Ball milling was performed by a planetary ball mill (Pulverisette 7, Fritsch, Germany). Typically, 23 mL of DMSO, varied amounts of n-dodecyl succinic anhydride or succinic anhydride, DMAP and cellulose were loaded to a 40 mL-zirconia pot containing seven 10-mm zirconia balls at room temperature. The rotation was 200 rpm, working time 20 min and interval of 2 min to avoid overheating. The milling time was varied from 2 h to 40 h.

Post-treatment

Succinic anhydride: After ball milling, cellulose was washed with DMSO, isopropanol and ethanol by centrifugation at 10000 rpm, 3 times each. The purified cellulose nanofiber was dispersed in water or DMSO by sonication for 20 min at various concentrations.

N-dodecyl succinic anhydride: The ball-milled sample was washed with o-xylene and ethanol 3 times each.

Preparation of cellulose nanofiber composite

20 g of polyethylene was dissolved in 2 L o-xylene at 130°C. The solution was mixed with the suspension of cellulose nanofiber originating from commercial pulp in o-xylene by vigorous stirring. After 10 min, the suspension was poured into acetone for precipitating solid. After washing by ethanol twice, the precipitate was vacuum dried at 105 °C. The resulting composite was melted in a mould at 150°C, hot pressed at 20 MPa for 5 min, and cooled in ambient atmosphere.

Determination of the degree of substitution

The carboxyl content of cellulose samples was determined by conductometric titration as follows: cellulose nanofiber suspension was mixed with 2 mL of 0.1 N HCl, followed by addition of 0.1 N NaOH at 0.1 mL/min. The change in conductivity was monitored by a conductometer. Then the suspension was dialyzed against water and freeze-dried for weighing.

$$DS = \frac{162\times (V_{NaOH}\times c_{NaOH})}{m - Y\times (V_{NaOH}\times c_{NaOH})} \quad (1)$$

Where: 162 g/mol is the molar mass of an anhydroglucose unit (AGU), Y (291.4 or 123.1) g/mol is increase in molecular weight of AGU by substitution of one OH group, *m* is dry weight of the sample, V_{NaOH} is the volume of NaOH solution consumed in titration, and c_{NaOH} is the molarity of NaOH solution.

Characterizations

Fourier transform infrared (FTIR) spectra were recorded using a Varian 3100 FT-IR spectrometer with 2 cm^{-1} resolution and accumulation of 24 scans.

X-ray photoelectron spectroscopy (XPS) spectra were obtained with ESCALAB220i-XL Photoelectron Spectrometer (VG Scientific). A Gaussian curve fitting program was used to treat the C1s signal and the following binding energies.

X-ray diffraction (XRD) patterns of the products were recorded using an X'Pert PRO X-ray diffractometer with CuKα radiation (λ=0.154184 nm).

Nitrogen adsorption–desorption measurements were carried out using a Quantachrome NOVA 4200e surface area analyzer at -199.7 ℃ by using the volumetric method. For this analysis the ball-milled sample wet with DMSO was solvent-exchanged to n-butanol and freeze-dried. The Brunauer–Emmett–Teller (BET) specific surface areas were calculated by using adsorption data in P/P_0=0.05–0.3 (six points collected).

Transparency was evaluated by a UV-vis spectrometer (Cary 5000) from 400 to 750 nm by introducing cellulose suspension into a quartz cuvette. A cuvette filled with DMSO or o-xylene was used as reference.

Scanning electron microscopy (SEM) observations were carried out using a JEOL JSM-6700F operated at accelerating voltage of 5 kV. The specimens were coated with gold by ion sputtering.

For transmission electron microscopy (TEM) observations, one drop of cellulose nanofiber in o-xylene or DMSO (0.01%w/v) was deposited on a carbon-coated grid. After drying under vacuum, they were observed using Hitachi H800 microscope operated at accelerating voltage of 100 kV.

Zeta potential measurement was carried on Zetasizer Nano ZS (Malvern) at 1% concentration with pH around 5.

Thermogravimetric analysis (TGA) was carried by a TA-Q50 (TA Instruments) from 100 to 500 °C at heating rate of 10 °C/min under N_2 atmosphere.

Tensile testing of the nanocomposite was carried out by using MTS Sintech-1 (MTS Systems) with a load cell of 50 lb following ASTM D 638. The crosshead speed was set to 50 mm/min. The samples were cut in a dumbbell shape with an ASTM D 638 (type V) die and at least five specimens were tested for each sample. The impact fracture testing was carried out by AJ U – 22, following ASTM D256. Five specimen for each composition were tested.

Result and discussion

Structure characterization

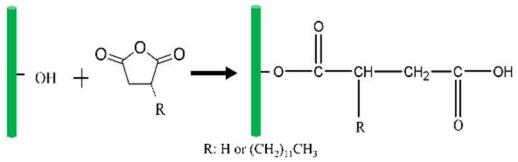

Figure 1. *Surface esterification of cellulose nanofibers*

In the defibrillation process by ball milling, hydroxyl groups on the surface of cellulose nanofiber undergo esterification with anhydride as illustrated in **Figure 1**, giving a free carboxyl group on the side chain.

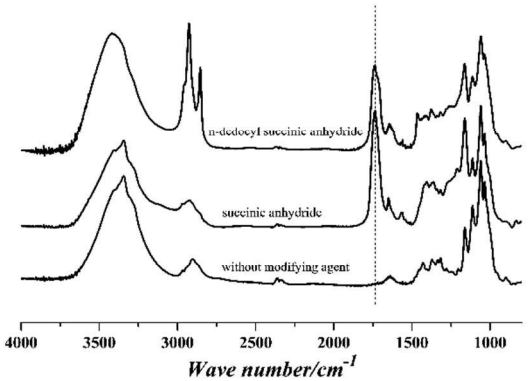

Figure 2*. FT-IR of cellulose nanofiber with and without surface modification.*

As shown in **Figure 2**, esterification by succinic anhydride is catalyzed effectively by DMAP as evidenced by the appear-

ance of new bands at 1740 cm^{-1}, 1573 cm^{-1} and 1165 cm^{-1}, stretching of carbonyl group and antisymmetric stretching of carboxylic anion, and C-O antisymmetric stretching, respectively. The absence of peaks at 1850 and 1780 cm^{-1} suggests that the products are free of unreacted succinic anhydride. The cellulose sample treated with n-dodecyl succinic anhydride shows increased peaks intensity of C-H stretching at around 2900 cm^{-1}, apparently due to the introduction of long alkyl chain. By comparison, there is no esterification detected even prolonging the time of ball milling up to 40 h at the absence of DMAP, indicating the essentialness of catalyst in this process.

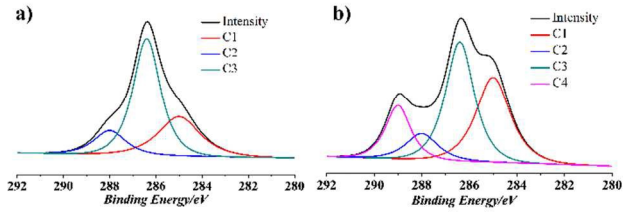

Figure 3. *XPS intensity as function of binding energy from C_{1S} spectra of cellulose nanofiber after modification. (C1: C-C, C-H, C2: C-O, C3: O-C-O, C4: O-C=O.)*

Additional evidence of the esterification between cellulose nanofiber and succinic anhydride was obtained by X-ray photoelectron spectroscopy (XPS). Results of curve-fitting for the C_{1S} region by using Gaussian function are shown in **Figure 3**. For the modified samples, a new peak ascribed to esters (O=C-O) could be separated at 289 eV, and the peak at 285 eV characteristic for C-C (C1) increased significantly due to the introduced alkyl groups, attesting the strong localization of ester groups on the surface of cellulose nanofiber. Although withstanding severe mechanical shear and chemical reaction, the original crystallinity was preserved and the integrity of crystalline cellulose was maintained (**Figure S1**).

Morphology and dispersibility of cellulose nanofiber

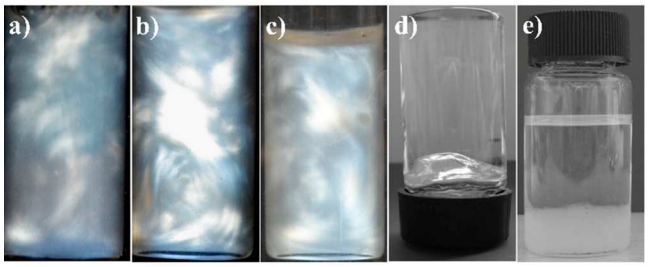

Figure 4. *Cellulose nanofiber suspensions from 20 h-ball milling with succinyl anhydride, after standing 2 day. Flow birefringence was observed through crossed polarizers. Medium: (a) water, (b) DMSO, (c) o-xylene. Cellulose nanofiber modified by n-dodecyl succinic anhydride dispersed in o-xylene forms gel (d). o-xylene suspension of unmodified cellulose nanofiber (e).*

The surface property of cellulose nanofiber can be tailored by the side chain. Modified by different types of anhydride, cellulose nanofiber presents different dispersibility. The succinylated cellulose nanofiber has carboxyl groups on the surface, and could be dispersed in polar liquids. As shown in **Figure 4a** and **4b**, the nanofiber suspensions in water and DMSO show flow birefringence through crossed polarizers, indicating high levels of individualization of cellulose nanofibers. The n-dodecyl succinylated cellulose nanofiber could be readily dispersed in o-xylene and shows flow birefringence (**Figure 4c**). After standing for 2 days, this suspension forms a gel (**Figure 4d**) while the unmodified cellulose nanofiber suspension precipitates immediately after powerful ultrasonic treatment (**Figure 4e**).

TEM images show high level of dispersion and preservation of nano-scale fibrillar morphology (**Figure 5**). Here again, effect of esterification is seen clearly by comparing **Figure 5b** and **5c**; while the material ball-milled without reagent consisted of severely disrupted fibrils and their aggregates, the esterified cellulose dried from DMSO shows nanofibers approx. 20 nm wide and several μm in length. Cellulose nanofiber modified by n-dodecyl succinic anhydride shows the similar morphology (**Figure 5d**), although bundles can be seen from the image, which is caused by the high boiling point of o-xylene and the long chain on the surface making cellulose nanofiber tend to entangle with each other during vaporization of o-xylene. The dimension of cellulose nanofiber is consistent with our previous work.

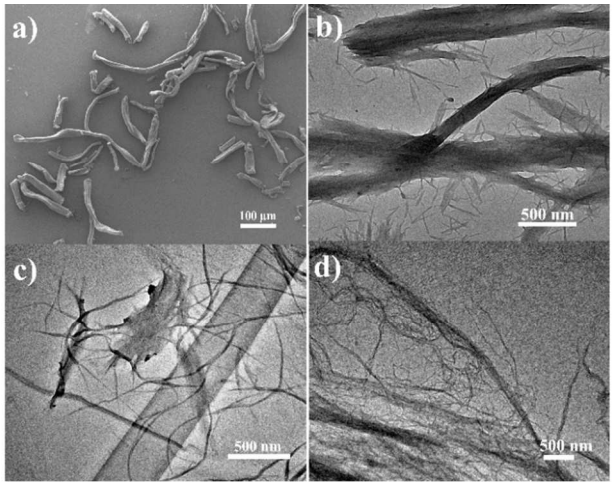

Figure 5*. SEM image of starting cellulose (a), and TEM image of unmodified cellulose nanofiber dispersed in DMSO (b), modified cellulose nanofiber dispersed in DMSO (c), and in* o-xylene *(d).*

Evolution of esterification

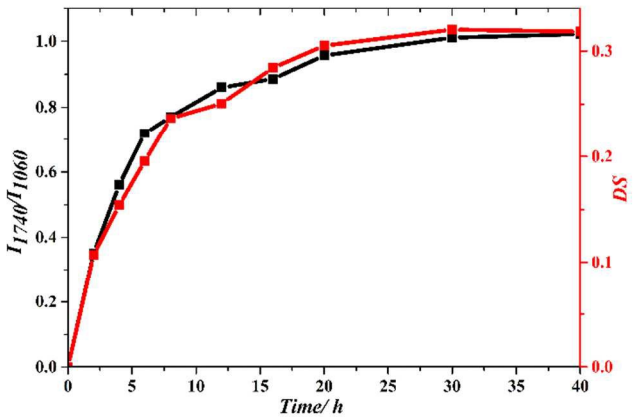

Figure 6. FT-IR *peak height ratio of the 1740 to 1060 cm^{-1}*

(I_{1740}/I_{1060}) and DS from titration vs. milling time for cellulose nanofiber reacted with succinic anhydride.

The degree of substitution (DS) was determined by conductometric titration of carboxyl group introduced by esterification. Thus determined DS was chosen to establish calibration of FT-IR data for easier determination of DS. In **Figure 2**, the C-O stretching peak of glucopyranoside at 1060 cm^{-1} is not affected by esterification, and the new peak at 1740 cm^{-1} of C=O stretching appears after esterification. **Figure 6** shows good correlation between the DS values by the two methods. Thus, the ratio I_{1740}/I_{1060}, can be used to determine DS by using the following equation.

$$DS=0.31*(I_{1740}/I_{1060}) \quad (2)$$

The DS by succinic anhydride increases steeply in the first 10 h, then gradually levels off. The maximum DS of 0.31 was attained after 30 h. The reaction with n-dodecyl succinic anhydride follows a similar pattern, giving maximal DS of 0.23 by 40 h of ball-milling **(Figure S2a)**. These DS values are lower than that for hexanoyl chloride, 0.58. This difference can be ascribed to lower reactivity of anhydrides, and steric hindrance by n-dodecyl group and the catalyst DMAP[11].

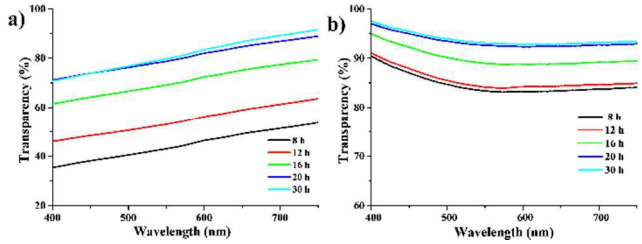

Figure 7. UV-vis transmittance of surface-esterified cellulose nanofiber suspensions in DMSO (a) and o-xylene (b).

The relationship between milling time and level of dispersion was examined by UV-vis transmittance. Figure 7 shows that prolonged ball milling results in higher transparency. The maximum transparency is attained at 20 h milling, after which there was little further changes. This behavior is parallel with the change in DS, suggesting that dispersibility is governed by the degree of surface esterification.

With the use of acylation catalyst DMAP[12], disintegration of cellulose nanofiber determines the evolution of esterification. The change in DS is consistent with the change of specific area of cellulose ball milling in DMSO without surface modification (**Figure S3**), suggesting efficient disintegration would lead to higher level of surface esterification. Based on the observed behavior, 20 h milling was chosen as standard condition for the following examination of the influences of reagent and catalyst doses.

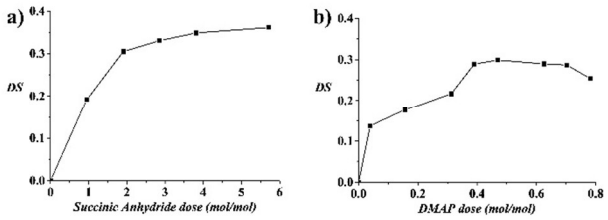

***Figure 8.** DS as a function of different content of succinic anhydride (a) and DMAP (b).*

Figure 8a shows that the DS of product increases with increase in succinic anhydride dose, levelling off at approx. 0.35. Therefore the anhydride dose of 2 mol/mol glucopyranoside unit could be chosen as standard condition. Figure 8b shows the influence of catalyst (DMAP) dose on the product's DS. The curve is not monotonous, showing decline in DS at above 0.7 mol/mol. The results for n-dodecyl succinic anhydride and DMAP on DS showed similar tendencies (Figure S2b and 2c).

Besides high versatility, one advantage of current method is high yield of processed cellulose. **Table 1** shows the recovery of cellulose nanofiber modified by succinic anhydride and n-dodecyl succinic anhydride as 78.1% and 81.3%, respectively, both higher than that of cellulose nanofiber modified by hexanoyl chloride (73%)[9]. The corresponding FTIR spectrum are shown in **Figure S4**. A possible cause of this difference is that hexanoyl chloride can form free acid more easily, which decomposes cellulose to small soluble species.

***Table 1**. Yield and DS of cellulose nanofibers.*

Cyclic anhydride		Weight percentage (%)	DS
Succinic anhydride	Insoluble	78.1	0.30
	Soluble	21.9	0.51
N-dodecylsuccinic anhydride	Insoluble	81.3	0.23
	Soluble	18.7	0.45

Thermal property of cellulose nanofiber

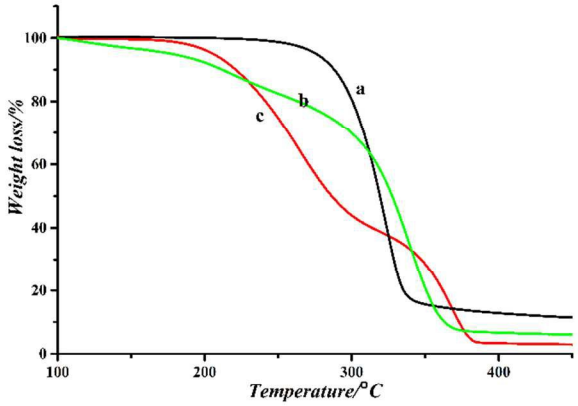

***Figure 9.** TGA in nitrogen of cellulose nanofiber (a) and modified by succinic anhydride (b) and N-Dodecyl succinic anhydride (c).*

Thermogravimetry in nitrogen (**Figure 9**) shows significant low-temperature shift of the surface-esterified cellulose nanofibers compared with the original cellulose. Weight loss of the

esterified products starts at below 200 °C, against approx. 250°C for unmodified cellulose. This difference can be ascribed to decomposition and vaporization of the ester groups. The TGA curves of esterified products show two-stage weight losses. The first stage starts at around 175 °C, which could be ascribed to decomposition of ester linkages; the second stage starts at around 285°C similar to that of unmodified cellulose arising from decomposition of cellulose backbone. The larger weight loss in the first stage of n-dodecyl succinated cellulose is ascribed to the larger size of the ester group. The decrease in thermal stability may be caused by the presence of free carboxyl group on the surface, catalyzing the decomposition of cellulose. Similar results have been reported in cellulose nanocrystal hydrolyzed by sulfuric acid[13].

Surface property of cellulose nanofiber

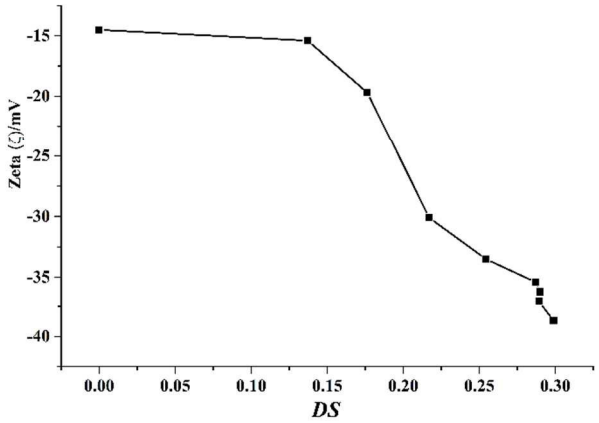

Figure 10. *Zeta potential of cellulose nanofiber modified by succinic anhydride*

Due to the presence of free carboxyl group introduced by ring-opening esterification, electrostatic repulsion provides stable dispersion of the cellulose nanofibers in water. **Figure 10** shows the change in zeta potential of the nanofibers by surface succinylation with strong correlation with DS. Cellulose nanofiber with DS of 0.3 has a decreased zeta potential of -38.7 mV while the original cellulose nanofiber has a zeta potential around -14.7 mV. The increase in negative charge would result in improved dispersion stability in water.

Table 2. *Tensile test of cellulose reinforced PE nanocomposite.*

Content of CNF (%)	Tensile strength (MPa)	Young's modulus (GPa)
0	35	4.32
1	40.8	6.39
2	44.6	7.59
3	44.7	7.93
5	44.7	6.45
10	40	5.83

Modified by n-dodecyl succinic anhydride, cellulose nanofiber shows improved compatibility with PE. The resulting cellulose nanofiber could be homogenously mixed with PE in o-xylene forming transparent suspension, which were dry-cast to form film specimens. This nanocomposite film showed remarkable enhancement of mechanical properties compared with neat PE. **Table 2** shows the changes in tensile strength and Young's modulus of the composite by increasing cellulose nanofiber content. Young's modulus increased sharply and reaches 7.93 GPa at 3% cellulose loading, approx. 83% increase from neat PE, but further increase of loading caused decrease of Yong's modulus. The tendency is similar for tensile strength, which has approx. 28% increase at the load of 3% cellulose nanofiber. SEM observation of fractured surface of the composites showed good dispersion of nanofibers in the matrix, though with certain level of inhomogeneities (**Figure S5**).

The improved adhesion between the matrix and the filler would contribute to better stress transfer from the matrix to rigid cellulose nanofibers. The mechanical performances decline by over 3% cellulose loading, when cellulose nanofibers begin to entangle with each other and form large aggregates. In comparison, unmodified cellulose nanofiber was not homogenously dispersed in PE matrix, forming aggregates at the load of 1% (**Figure S5e** and **S5f**), this result is consistent with **Figure 4e** in which cellulose nanofiber precipitates immediately in o-xylene, indicating poor compatibility with polyethylene.

Conclusion

Surface esterification-dispersion of cellulose nanofiber is possible by ball milling native cellulose with cyclic anhydrides of organic acids. The reaction is catalyzed by DMAP effectively. The resulting cellulose nanofibers are 15-20 nm wide and several micrometers long. We found that ball milling in organic solvents with reactive chemicals has a dramatic effect in nanoscale dispersion and surface derivatization of cellulose. Through the change of anhydride, the produced cellulose nanofibers show different surface property. The succinylated nanofiber can be stably dispersed in water with zeta potential up to -38.7 mV at pH=5.5. The n-dodecyl succinylated nanofiber can be dispersed in o-xylene, from which polyethylene-cellulose nanocomposites were prepared. Compared with neat polyethylene, nanocomposite with optimal composition of 3% cellulose owed Young's modulus of 7.93 GPa (83% increase) and tensile strength of 44.7 MPa (28% increase). While solution casting is not a practical way for nanocomposite manufacturing, the improved compatibility of the nanofibers demonstrated here would also be effective in melt processing. These results demonstrate versatility of ball mill processing of cellulose for fabricating various functionalized cellulose nanofibers. This method would also be applicable to other materials and purposes that involve heterogeneous processing.

ACKNOWLEDGMENT

This work was supported by the National Program on Key Basic Research Project (973 Program, No. 2011CB933700), the National Natural Science Foundation of China (No. 51472253, 51373191, 51172247), and the Chinese Academy of Sciences Visiting Professorships.

Supporting Information Available: The material is available free of charge via the Internet at http://pubs.acs.org.

REFERENCES

1. Eichhorn, S.; Dufresne, A.; Aranguren, M.; Marcovich, N.; Capadona, J.; Rowan, S.; Weder, C.; Thielemans, W.; Roman, M.; Renneckar, S. Review: current international research into cellulose nanofibres and nanocomposites. *Journal of Materials Science* **2010,** *45* (1), 1-33.

2. (a) Tingaut, P.; Zimmermann, T.; Lopez-Suevos, F. Synthesis and Characterization of Bionanocomposites with Tunable Properties from Poly(lactic acid) and Acetylated Microfibrillated Cellulose. *Biomacromolecules* **2009,** *11* (2), 454-464; (b) Mendez, J.; Annamalai, P. K.; Eichhorn, S. J.; Rusli, R.; Rowan, S. J.; Foster, E. J.; Weder, C. Bioinspired Mechanically Adaptive Polymer Nanocomposites with Water-Activated Shape-Memory Effect. *Macromolecules* **2011**, null-null.

3. (a) Klemm, D.; Kramer, F.; Moritz, S.; Lindström, T.; Ankerfors, M.; Gray, D.; Dorris, A. Nanocellulosen: eine neue Familie naturbasierter Materialien. *Angewandte Chemie* **2011,** *123* (24), 5550-5580; (b) Eichhorn, S. J. Cellulose nanowhiskers: promising materials for advanced applications. *Soft Matter* **2011,** *7* (2), 303-315; (c) Fukuzumi, H.; Saito, T.; Iwata, T.; Kumamoto, Y.; Isogai, A. Transparent and High Gas Barrier Films of Cellulose Nanofibers Prepared by TEMPO-Mediated Oxidation. *Biomacromolecules* **2008,** *10* (1), 162-165; (d) Mahmoud, K. A.; Male, K. B.; Hrapovic, S.; Luong, J. H. T. Cellulose Nanocrystal/Gold Nanoparticle Composite as a Matrix for Enzyme Immobilization. *ACS Applied Materials & Interfaces* **2009,** *1* (7), 1383-1386; (e) Dong, S.; Roman, M. Fluorescently labeled cellulose nanocrystals for bioimaging applications. *Journal of the American Chemical Society* **2007,** *129* (45), 13810-13811; (f) Huang, J.; Ichinose, I.; Kunitake, T. Biomolecular modification of hierarchical cellulose fibers through titania nanocoating. *Angewandte Chemie International Edition* **2006,** *45* (18), 2883-2886.

4. Alemdar, A.; Sain, M. Biocomposites from wheat straw nanofibers: Morphology, thermal and mechanical properties. *Composites Science and Technology* **2008,** *68* (2), 557-565.

5. (a) Gindl, W.; Keckes, J. All-cellulose nanocomposite. *Polymer* **2005,** *46* (23), 10221-10225; (b) Nishino, T.; Matsuda, I.; Hirao, K. All-Cellulose Composite. *Macromolecules* **2004,** *37* (20), 7683-7687; (c) Soykeabkaew, N.; Nishino, T.; Peijs, T. All-cellulose composites of regenerated cellulose fibres by surface selective dissolution. *Composites Part A: Applied Science and Manufacturing* **2009,** *40* (4), 321-328.

6. Mondragón, M.; Arroyo, K.; Romero-García, J. Biocomposites of thermoplastic starch with surfactant. *Carbohydrate Polymers* **2008,** *74* (2), 201-208.

7. Ljungberg, N.; Cavaillé, J. Y.; Heux, L. Nanocomposites of isotactic polypropylene reinforced with rod-like cellulose whiskers. *Polymer* **2006,** *47* (18), 6285-6292.

8. (a) Ifuku, S.; Nogi, M.; Abe, K.; Handa, K.; Nakatsubo, F.; Yano, H. Surface modification of bacterial cellulose nanofibers for property enhancement of optically transparent composites: dependence on acetyl-group DS. *Biomacromolecules* **2007,** *8* (6), 1973-1978; (b) Cavaille, J.-Y.; Chanzy, H.; Fleury, E.; Sassi, J.-F. Surface-modified cellulose microfibrils, method for making the same, and use thereof as a filler in composite materials. Google Patents: 2000.

9. Huang, P.; Wu, M.; Kuga, S.; Wang, D.; Wu, D.; Huang, Y. One‐Step Dispersion of Cellulose Nanofibers by Mechanochemical Esterification in an Organic Solvent. *ChemSusChem* **2012,** *5* (12), 2319-2322.

10. Fidale, L. C.; Ruiz, N.; Heinze, T.; Seoud, O. A. E. Cellulose Swelling by Aprotic and Protic Solvents: What are the Similarities and Differences? *Macromolecular Chemistry and Physics* **2008,** *209* (12), 1240-1254.

11. Liu, C.; Zhang, A.; Li, W.; Sun, R. Chemical Modification of Cellulose with Succinic Anhydride in Ionic Liquid with or without Catalysts.

12. Sun, R.; Fanga, J.; Tomkinson, J.; Hill, C. Esterification of hemicelluloses from poplar chips in homogenous solution of N, N-dimethylformamide/lithium chloride. *Journal of wood chemistry and technology* **1999,** *19* (4), 287-306.

13. Leung, A. C. W.; Hrapovic, S.; Lam, E.; Liu, Y.; Male, K. B.; Mahmoud, K. A.; Luong, J. H. T. Characteristics and Properties of Carboxylated Cellulose Nanocrystals Prepared from a Novel One-Step Procedure. *Small* **2011,** *7* (3), 302-305.

Pei Huang, Yang Zhao, Shigenori Kuga, Min Wu*, Yong Huang*

A versatile method to fabricate functionalized cellulose nanofiber and its application

Individual dispersed cellulose nanofiber can be produced through ball milling by adding anhydride and DMAP in one step. By altering the type of anhydride, cellulose nanofiber presents different surface property, making cellulose nanofiber compatible various solvent or matrix. This method sheds a light on the massive application of cellulose nanofiber.

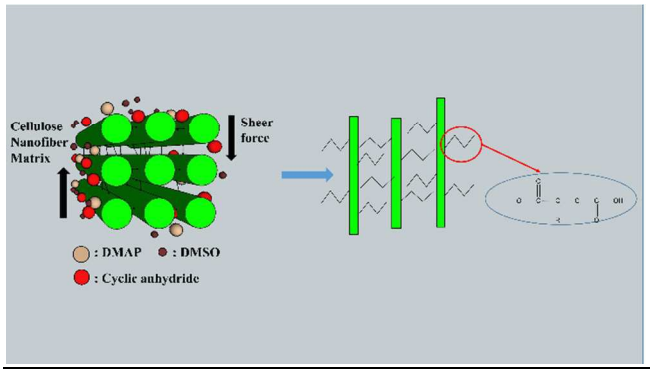

Table of Contents